ICONHIC 2016
1st International Conference on Natural Hazards & Infrastructure
28-30 June, 2016, Chania, Greece

Experiments on Tsunami Impact with a Vertical Sea Wall

D. J. McGovern[1], T. Robinson[2] and T. Rossetto[3]
University College London

ABSTRACT

The impact of tsunami with a vertical sea wall is examined in a series of large scale physical model tests. Of interest to the design engineer is the maximum value and time-history of the force and moments recorded at the wall for a given tsunami wave amplitude and period. This paper presents preliminary selected results from an extensive test programme. Scaled trough-led tsunami periods ranging between approximately 17 – 79 s are generated using a pneumatic long-wave generator. The waves impact a model vertical sea wall which is instrumented with an array of pressure transducers and a multi-axis load cell. The maximum and time-history of the loading is recorded. The results show breaking waves impart dynamic loads while longer non-breaking waves impart a hydrostatic load. The strongest positive correlations between the wave parameters and the maximum force and moment was with amplitude. Weaker negative correlations with wavelength are observed. Potential energy does not appear to influence the force which is proposed to be due to the distribution of the energy in the waveform, implying wave steepness is more important.

Keywords: Tsunami, Wall, Force, Pressure

INTRODUCTION

Tsunami are very long translator waves generated by a variety of mechanisms including vertical seafloor displacement that occurs during undersea thrust-fault earthquakes. Upon reaching continental shelf seas the tsunami waveform can shoal to a very large amplitude that may impact a sea wall. In designing such sea walls, the engineer requires knowledge of the impact force. During the Tohoku Earthquake and Tsunami of 2011, damage to sea walls was extensive and in many cases constituted total failure (EEFIT 2011, ASCE-COPRI-PARI., 2013 and Mori et al., 2012). Diverse failure modes were observed retrospectively including sliding and/or overturning, scour of the rear toe foundation and high velocity flows through wall member joints undermining the structures integrity. Raby et al., (2015) give a review of the Tohoku Tsunami interaction with coastal defences. Post 2011 the two-level tsunami hazard classification was implemented by the Japanese authorities based on return period and inundation depth at a particular location (Shibayama et al., 2013). All coastal defences must now defend a level 1 event (return period 50 – 60 to 150 – 160 years typically 7 – 10 m inundation height) and remain structurally intact during a level 2 event (return period few hundred to a few thousand years > 10 m, encompassing up to 20 – 30 m inundation height). The revised PHB, (2014) technical standard suggests tsunami load is numerically modelled for a particular site, which if unavailable other, undefined methods ought to be used. It is presumed, therefore, the engineer would be forced to turn to empirical predictor equations based on laboratory data and or historical field data, both of which are scarce and incomplete. The NILIM (2013) disaster scenario manual provides further guidance on tsunami effects on coastal structures and recommendations of their design. The inclusion of design features such as armouring at

[1] Corresponding Author: D.J. McGovern, *University College London, d.mcgovern@ucl.ac.uk*

[2] Author: T. Robinson, *University College London, t.robinson@ucl.ac.uk*

[3] Author: T. Rossetto, *University College London, t.rossetto@ucl.ac.uk*

the toe of the defence structure to prevent scour and the interlocking of all individual structural segments are already being implemented in new sea wall and defence builds in Japan (Raby et al., 2015). The forthcoming ASCE/SEI 7-10 (2016) chapter 'Tsunami Loads and Effects' constitutes a very important revision for tsunami design outside of Japan. However, it does not provide explicit guidance or methodology to predict the tsunami loading at a sea defence nor appropriate design guidelines. It appears, therefore, that the design engineer has relatively little guidance and typically little experience of tsunami induced loads on a sea wall, and as such is given few options other than the available methods developed for wind waves.

The loading of wind waves on a coastal structure is generally divided into 'pulstating' (non-breaking), 'impulsive' (shock impact from breaking waves) and broken waves. There are a multitude of methodologies for calculating maximal time-histories of loads and moments from waves on a coastal defence. Methods to calculate pulsating loads are well established (Goda, 1995). The most widely used method is that of Goda (1984), which assumes a trapezoidal distribution of wave pressure on the front of a vertical wall. This is integrated over its height to estimate the horizontal force. Minikin, (1963) developed and equation for predicting pressures from directly breaking waves on a vertical wall. The British Standard (BS6349-1, 2000) recommends Allsop and Vicinanza, (1996) for predicting impact loading on a vertical wall.

There is a growing data set available in the case of tsunami bore induced pressures at vertical walls with recent additions from Kihara et al., (2015) and Roberston et al., (2013). Tsunami bore are generally attributed to fissioned waves that overlie the longer period tsunami, sometimes formed as a result of a steep offshore bathymetry. They may induce large impulsive pressures but generally comprise only a fraction of the full loading time-history from a tsunami inundation. Post-bore, and in the absence of an initial bore, the quasi-static forces and quasi-steady velocities associated with the bulk of the tsunami will be very important parameters on the loading at a sea wall.

In order to better understand the full time-history of the loading from a tsunami on a sea wall, additional data is needed that encompasses the full inundation time of the tsunami. This paper presents a first look at selected preliminary results of a large scale experimental study of the tsunami load time-history on a sea wall. It should be viewed as a 'work-in-progress'. It is organised in the following way. The methodology describes the experimental facility and equipment. The selected results are presented in the results section, including example loading time-histories, the peak forces and overturning moments and the sensitivity of the force and moment recorded at the wall to the characteristic parameters of the incident wave. Finally, the conclusions are given.

METHODOLOGY

The experiments are carried out at HR Wallingford in the 100 m long and 1.8 m wide flume with an operating water depth d of 0.6 m ~ 1.0 m. Figure 1 presents a schematic diagram of the set-up. To generate scale tsunami-length waves a pneumatic methodology is employed based on the method described in Rossetto et al., (2011). The pneumatic long-wave generator is installed at the far end of the flume and at the opposite end a 1:20 sloping bathymetry is installed reaching a maximum height of 1 m. This is the nominal position of the shoreline and the toe of the model seawall. The scale of the tests is 1:50. The full range of wave periods T tested are from 6.5 – 230 s corresponding to 46 s – 27 min at prototype. This paper focuses on $T \approx 17 – 79$ s (2 min – 9.3 min). Where T is defined as the time difference between the start of the trough and the end of the crest as shown in figure (Figure 2). The positive amplitudes a^+ and negative amplitudes a^- are varied along with variations in the length of the troughs and crests.

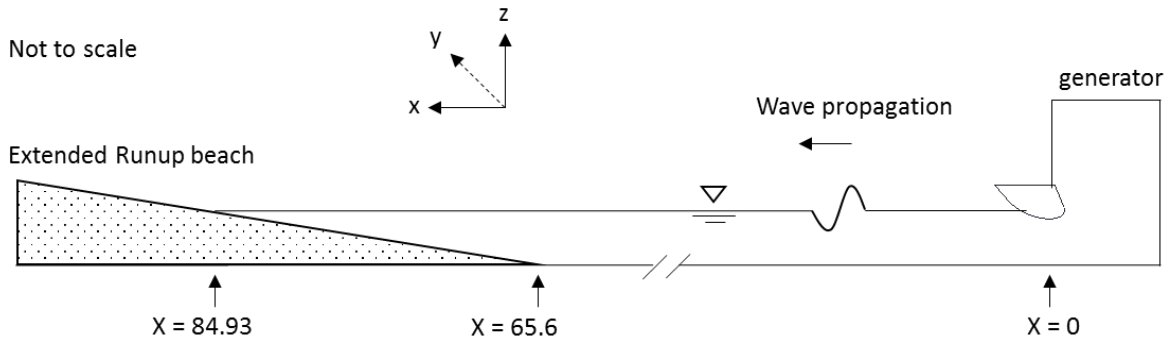

Figure 1. A schematic cross-sectional diagram of the flume (not to scale, distances in meters m).

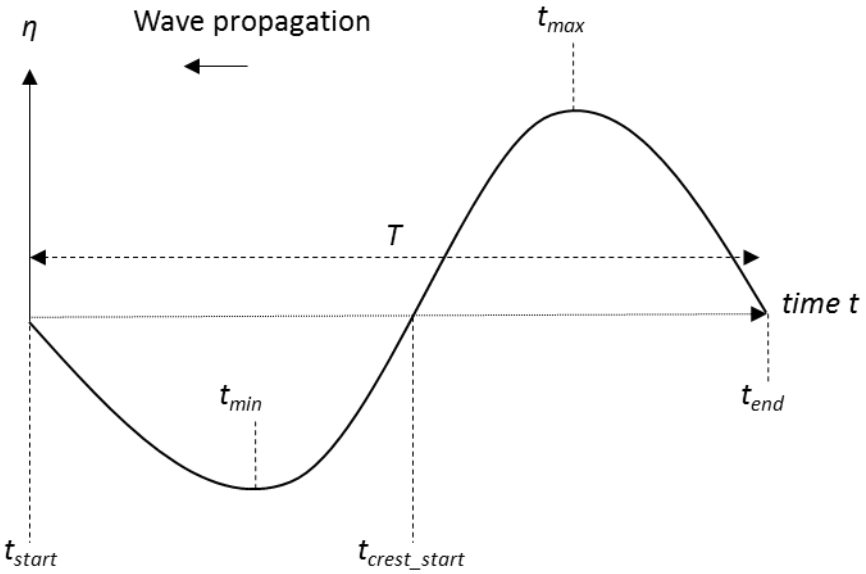

Figure 2. The definition of wave parameters.

Free-surface elevation η is recorded at various locations from X = 7.02 – 88.1 m in the offshore (constant depth region of the flume), the nearshore (above the sloping bathymetry) and onshore (extended beach) regions of the flume using 16 resistance-type wave gauges. These gauges are calibrated daily before testing. The celerity of the waves in the experiment C_{exp} is calculated from the temporal correlation of the beginning of waveform between the offshore and bathymetry toe wave gauges.

The vertical wall is 0.25 m high. The body force load is recorded using a Kistler 9327C piezoelectric 3-axis load cell. The cell is capable of recording +/- 1 mN changes in load in perfect conditions and is linear over its measurement range capacity. The load cell is housed within the immovable section of the wall and the responding wall segment is cantilevered off the load cell as shown in Figure 3. The horizontal loads F_x and vertical F_z are directly measured by the load cell as a voltage to which a calibration is applied. The calibration is performed in-situ using a weighted pulley system to define the coefficients of the load cells linear response. The pressure transducers (Figure 3) are laid out in four adjacent columns at the following heights for wall one z = 0.03 m (column 1), z = 0.0565 m (2), z = 0.0385 m (3), z = 0.0742 m (4), z = 0.0945 m (1), z = 0.1245 m (2), z = 0.1115 m (3), z = 0.1465 m (4), z = 0.1645 m (1), z = 0.1985m (2), z = 0.1815 m (3), z = 0.2215 m (4). The height of the water at the wall is measured using pressure transducers, video and wave gauges. The total pressure p_{total} per metre-run recorded by the transducers is estimated from (1) which extends the pressure to the full height h of the water by a linear fit at the wall at a particular time t. For recording the maximum pressures $t = t_{max}$ where t_{max} is the time when the maximum pressure is recorded. The F_x is then calculated over the same width w of the cantilevered segment, i.e., 0.1 m (2).

$$p_{total} = \int_0^h p(z)\, dz \qquad (1)$$

$$F_x = p_{total} * w \quad (2)$$

Where z is the height of the transducer up the wall and p is the recorded pressure at the transducer. The overturning moment M_z is estimated from (3).

$$M_z = w * \int_0^h p_k(z)\, z_k\, dz \quad (3)$$

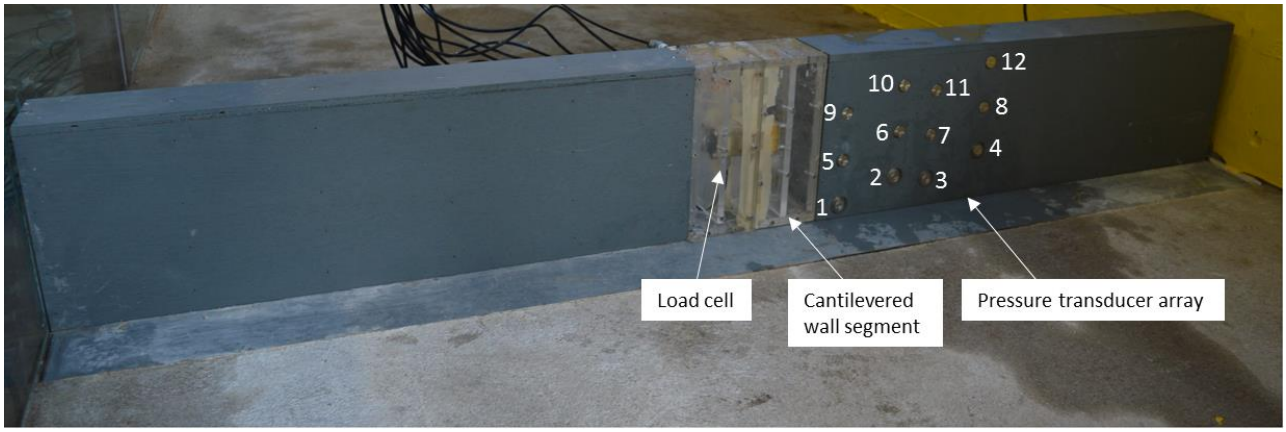

Figure 3. Annotated image of the 0.25 cm high, 0.1 cm wide vertical wall showing the load cell and pressure transducer set-up.

The potential energy E_p of the wave offshore is a relevant parameter in the description of tsunami runup on a sloping beach (e.g., Charvet et al., 2013 and McGovern et al., 2016). Reasonably, the force recorded on a coastal defence may also correlate with the E_p of the incident wave. In linear shallow water conditions E_p can be expressed as (4):

$$E_p = \int_0^T \frac{1}{2}\, g\rho\eta(t)^2 C\, dt \quad (4)$$

Where g = acceleration due to gravity, ρ = density of water, t = instantaneous time and C = wave celerity (calculated from the temporal correlation of the wave between the probes at the bathymetry toe adjacent in the offshore region).

RESULTS

Time-History of the Loading Event

This section details the time-history of the loading event, identifying its key characteristics chronologically. Figure 4a-b shows two typical impact loading profiles of the normalised period t_{total}/T (where t_{total} = total duration time of the impact event at the wall) as a function of normalised force $F_x/\rho gwHd$ (where H = offshore wave height, and d = still water level at the wall).

Figure 4a shows an impulse load profile at the wall from a breaking wave of T = 18 s. Video image stills are shown in Figure 4a-d. The impulsive load is manifest as a large and very brief spike at the start of the profile. The quasi-static load component is characterised by a double peak which is characteristic of the loading of both breaking and non-breaking wind waves. This quasi-static loading profile is well observed in wind wave breaking at or near sea walls (for example, Cuomo et al., 2010 and Peregrine, 2003). It differs from the loading time-history profile of a purely pulsating wave. A typical pulsating quasi-static profile from a T = 55 s wave is shown in Figure 4b, (video image stills are shown in Figure 5e-h.). In the absence of wave breaking, the loading profile is solely quasi-static. It rises to a maximum approximately 1/4 of the way into the loading event. The force then steadily drops with the recession of the wave off the wall. An important note of the quasi-steady pulsating force is that the wave appears to behave like a slosh. There is little observational (video and velocity

measurements) evidence of surging for the longer periods. This data will be discussed in greater detail in an upcoming journal publication which will address the full range of periods tested $T \leq 230$ s.

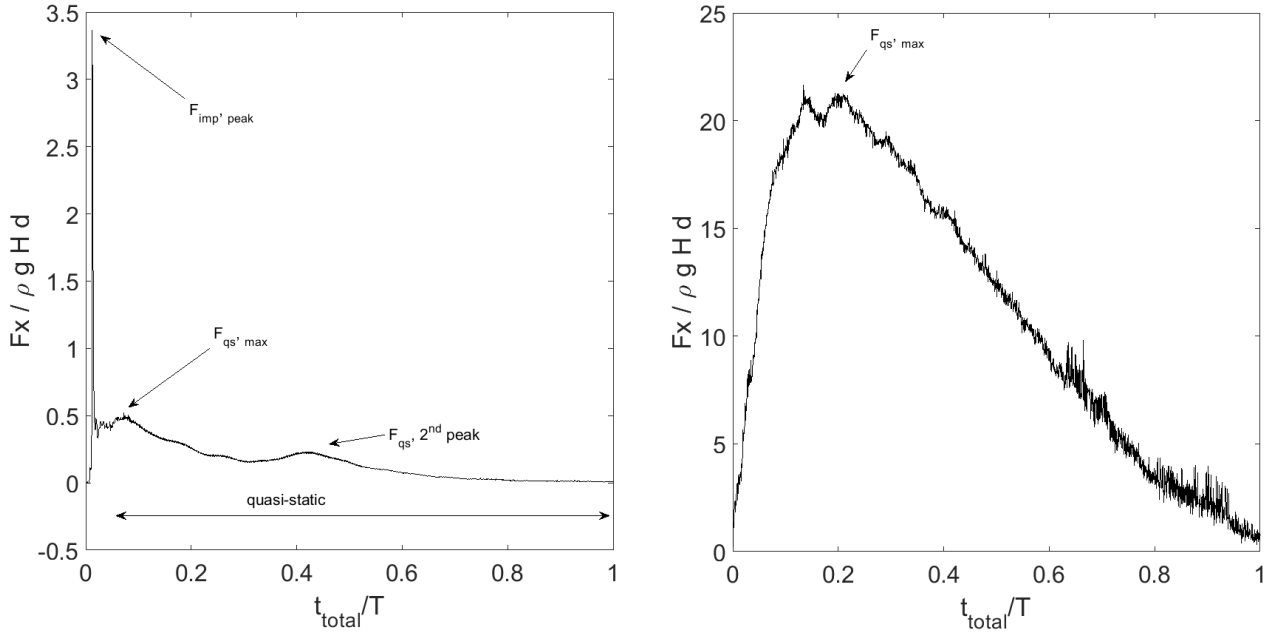

Figure 4a-b. Examples of the wave impact time history load recorded during the tests of a near directly breaking impact (Figure 4a, T = 18 s) and an unbroken pulsating quasi-static impact (Figure 4b, T = 55 s).

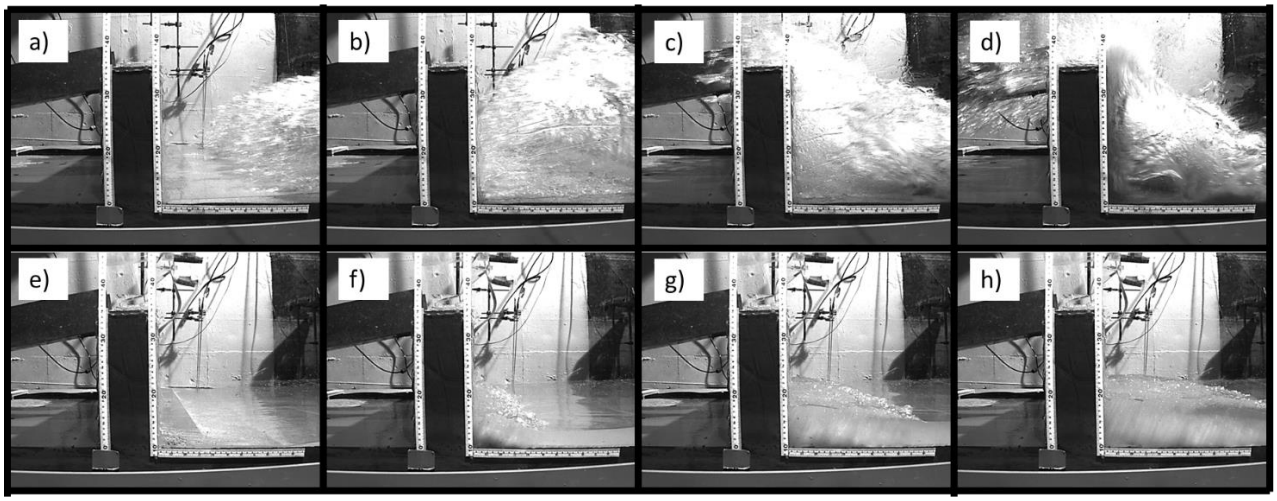

Figure 5a-h. High-speed video stills of the approach to and impact of the waves on the wall recorded during the tests. Figure 5a-d shows the broken wave impact shown in Figure 4a and Figure 5e-h an unbroken quasi-static impact shown in Figure 4b.

Figure 6 shows the maximum horizontal force $F_{x,max}$ from different types of impact, being either quasi-static (i.e., hydrostatically dominated) or impulsive impact (dynamic) as a function of T. Dynamic or impulsive force from high fluid velocity is generally suggested to be an important contribution to tsunami loads on walls (for example, Yeh, 2006). It is clear that the wave periods of lengths that are more relevant to tsunami that are produced in these tests are dominated by quasi-static loading. While the pulsating force is generally lower than an impulsive force, it has a longer duration, lasting over the entire crest period of the wave, and as such the time history of the quasi-static load is also an important quantity. A third type of impact which is observed in the data presented here (the images are withheld in this paper for brevity), is that of a surge. In such cases, the wave does not break prior to impact but clearly is steep enough to surge. There is a resulting dynamic impact that may be comprised of several maxima before the quasi-static component begins. This data will be discussed in a future publication.

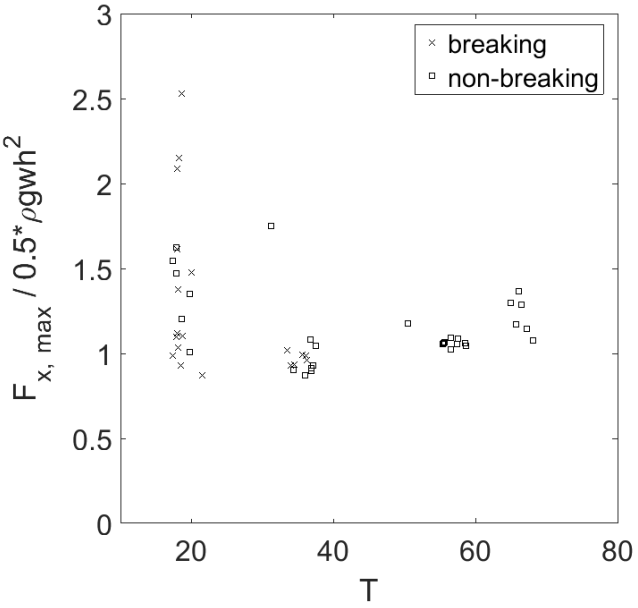

Figure 6. $F_{x,\,max}$ normalised with $0.5\rho gwh^2$ as a function of T.

Peak Forces and Overturning Moments

Focusing now on unbroken wave impacts, in this section the peak force and moments recorded at the wall are described. The analysis is carried out in order to understand the physical basis of the loading process in more detail. Figure 7 (a-d) presents $F_{x,\,max}$ as a function of T and H (a, c) and M_z (b, d) as a function of T and H for the non-breaking waves. There is a clear correlation between both T (negative) and H (positive) with $F_{x,\,max}$. The correlations are opposite because the volume of water in the pneumatic generator is finite. This limits the maximum a^+ of longer waves, the crests of which have a much larger volume than a shorter wave of equivalent a^+. The apparent quadratic relationship between H and $F_{x,\,max}$ is expected due to the hydrostatically dominated nature of the impacts of these unbroken waves.

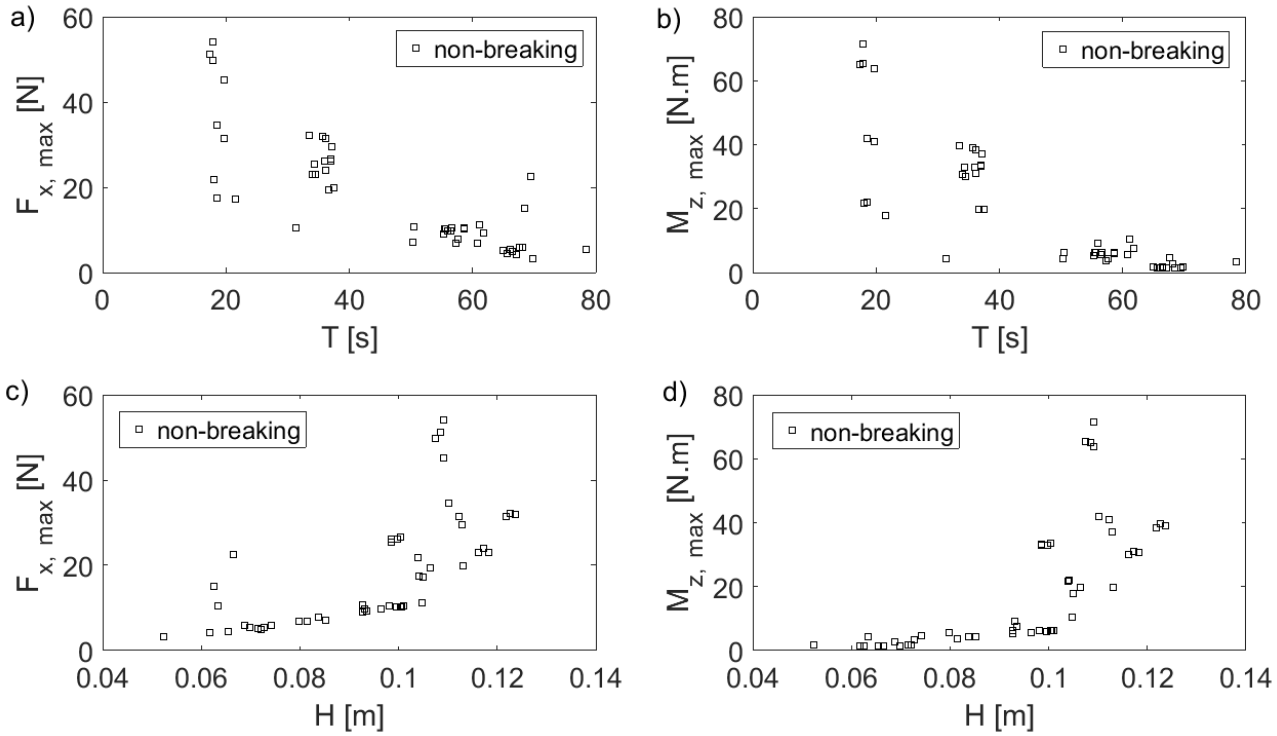

Figure 7a-d. Figure 7a and b present F_x as a function of T and H respectively while Figure 7c and d present M_z as a function of T and H respectively.

Sensitivity of the Force and Moment to Wave Parameters.

To determine the sensitivity of $F_{x,\,max}$ and $M_{z,\,max}$ with the wave characteristics, these values as recorded at the wall are plot as a function of a^+, a^-, wavelength λ, trough length λ_{tr}, crest length λ_{cr}, potential energy of the trough E_p^-, potential energy of the crest E_p^+, E_p and d. Figure 8 a-i presents the correlation plots for the non-breaking waves. a^+ is strongly positively correlated with $F_{x,\,max}$ which may be expected, as a larger amplitude offshore leads to a larger water level at the wall, and the load from unbroken waves is essentially hydrostatic. a^- is very weakly negatively correlated suggesting it is less important. λ, λ_{tr} and λ_{cr} all show negative correlations, indicating that longer length values are associated with smaller forces. This is expected as in these test generally the longer the wave the lower the a^+ which is related to the limited volume capacity of the pneumatic generator. d shows no correlation. E_p^-, E_p^+ and E_p shows little evidence of correlation with some of the highest loads correlating with the lower energies. This implies that E_p is not as important as a^+ for these long waves.

Considering that a very long wave of a given amplitude will have a given E_p that will depend on its length and free surface elevation over that length. A shorter wave with the same amplitude will have a lower E_p, due to its smaller length. However, it may shoal to a larger height at the wall as its initial offshore λ is smaller. The breaking criterion is often described using the wave steepness parameter a/λ. As for very long waves the denominator λ is several orders of magnitude greater than the numerator a, the reciprocal λ/a is used here for easier interpretation (Figure 9). A significant increase in $F_{x,\,max}$ with λ/a is observed. Describing runup tests conducted in the same facility as the present tests, McGovern et al., (2016) observe that the shoaling of T > ~80 s is negligible; the offshore amplitude is essentially the same as the maximum runup of the wave. Thus the regime of shoreline impingement for longer waves is different than for shorter ones. In the case of impacts with a sea wall, shorter waves can be hypothesized to exhibit some fluid acceleration from breaking and surging onto the wall which will lead to a larger force. This is opposed to the slow rise in water level induced by the longer wave impingement where the fluid velocity is too small to generate a dynamic pressure. This component is important for broken waves, such as tsunami bores, however, the majority of the loading is over the rest of the wave crest period. This loading is hydrostatically dominated. This will be explored further in an upcoming publication with the full data set available from these tests.

The sensitivity of the maximum calculated $M_{z,\,max}$ at the wall with the various wave parameters shows the distribution is much the same as for $F_{x,\,max}$ as expected (figure not shown here for brevity).

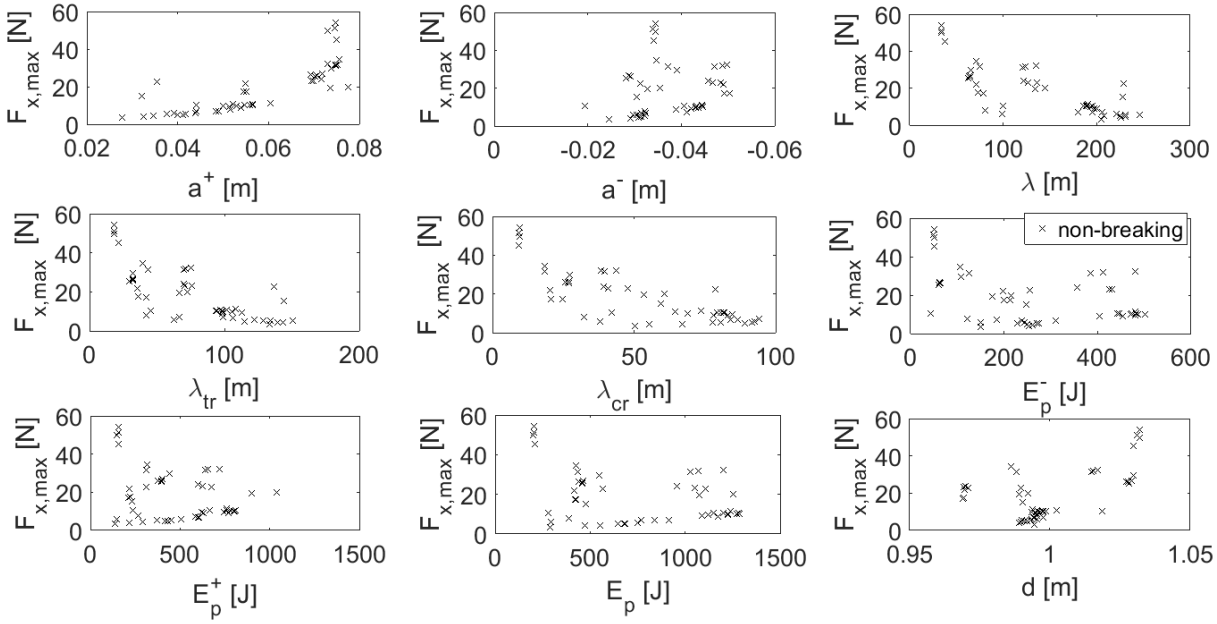

Figure 8. Correlation plots of $F_{x,max}$ as a function various wave parameters for the non-breaking waves .

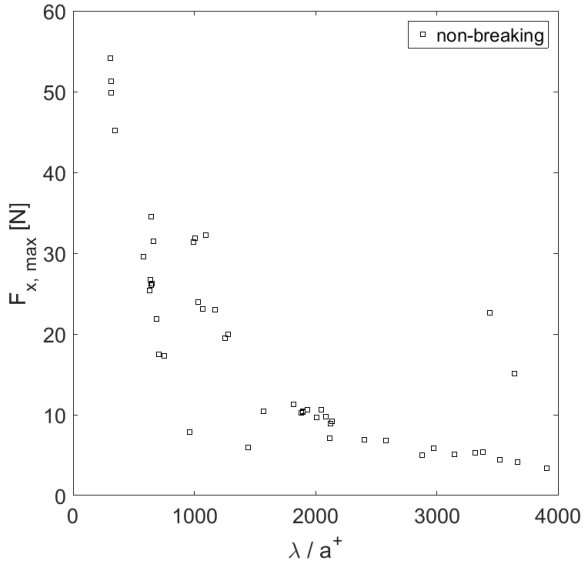

Figure 9. $F_{x,\,max}$ as a function of λ/a^{+} for the non-breaking waves (black crosses).

CONCLUSIONS

This paper presents the preliminary results of a selection of long, trough-led N-wave impacts with a vertical sea wall. The periods presented range from 6.5 – 79 s. The pressure and body force is recorded using an array of pressure transducers and a 3-axis load cell.

The results showed that waves that break before the wall impart higher, dynamic loads on to it. However, longer waves do not break and as such the loading is essentially a pulsating hydrostatic impact. The sensitivity analysis indicated strong positive correlations with amplitude, and weaker negative correlations with wavelength and maximum force at the wall. Potential energy did not correlate well and it is postulated that this is due to the distribution of the energy in the waveform. The implication is that wave steepness is more important. The data presented indicates that in the absence of breaking, the tsunami load is dominated by the hydrostatic load.

This is a first look at an extensive data set and due to their empirical nature it is unwise, therefore, to make any firm conclusions. An upcoming publication which contains more thorough treatise that encompasses the full data set from this extensive test programme will, it is hoped, allow firmer conclusions and design recommendations to be made

ACKNOWLEDGEMENTS

This work is fully funded by the URBAN WAVES ERC Starting Grant: 336084. The experiments use the 2nd generation Tsunami Simulator developed and constructed by HR Wallingford and operated onsite at HR Wallingford. The input of other researchers to these experiments is gratefully acknowledged. In no specific order: Prof. William Allsop of HR Wallingford, Prof. Ian Eames, Dr Christian Klettner, Dr Tristan Robinson, Dr Andrew Foster, Dr Crescenzo Petrone and Mr Oliver Cook, all Department of Civil, Environmental and Geomatic Engineering, University College London, Mr Ignacio Barranco Granged of the Department of Civil and Environmental Engineering, National University of Singapore and Dr Ingrid Charvet of Risk Management Solutions.

REFERENCES

Allsop NWH and Vicinanza D. Wave impact loadings on vertical breakwaters: development of new prediction formulae. *Proceedings of the 11th International Harbour Congress*, 1996, 275-284, Royal Flemish Society of Engineers, Antwerp, Belgium.

ASCE-COPRI-PARI. Coastal Structures Survey Team. Tohoku, Japan, Earthquake and Tsunami of 2011. eds. Ewing L. Takahashi S. and Petroff CM. 2013; *ASCE*

ASCE/SEI 7-10 Chapters 6-7 Tsunami Loads and Effects. *Minimum Design Loads for Buildings and Other Structure*s, 2016 ASCE.

British Standards. Maritime Structures Part 1: Code of Practice for General Criteria. *BS6349-1,* 2000, BSI, London, U.K.

Cuomo G, Allsop W, Bruce T, and Pearson J. Breaking wave loads at vertical seawalls and breakwaters. *Coastal Engineering*, 2010, 57; 424-439.

EEFIT. The Mw9.0 Tōhoku Earthquake and Tsunami of 11th March 2011: *A Field Report by EEFIT*. ⟨http://www.istructe.org/webtest/files/1d/1d158684-b77b-4856-99f8-2522fa25533b.pdf⟩, 2011.

Goda Y. *Random Seas and Maritime Structures*. 1985. University of Tokyo Press, Tokyo.

Goda Y. Japans Design Practice in Assessing Wave Forces on Vertical Breakwaters. Chapter 6 in *Wave Forces on Inclined and Vertical Wall Structures*. 1995. Eds. Kobayashi N. and Demirbilek Z. ASCE, New York.

Kihara N. Niida Y Takabatake D. Kaida H. Shibayama A. and Miyagawa Y., Large-scale experiments on tsunami-induced pressure on a vertical tide wall. *Coastal Engineering*, 2015, 99; 46–63

McGovern DJ. Chandler ID. And Rossetto T. Experimental Study of Tsunami Waves on a Smooth Sloping Beach. *Proceedings of the 6th International Conference on the Application of Physical Modelling in Coastal and Port Engineering and Science (Coastlab)*, 2016, May 10-13, Ottawa, Canada.

Minikin RR, Winds Waves and Maritime Structures. *2nd Edition*, 1963, Griffin, London.

Mori N. Takahashi T. and The 2011 Tohoku Earthquake Tsunami Joint Survey Group. Nationwide post event survey and analysis of the 2011 Tohoku earthquake tsunami. *Coastal Engineering Journal*, 2012, 54; (01), 1–27.

NILIM. A Draft Manual for Developing Earthquake-Tsunami Disaster Scenarios Including Damage to Public Works. ⟨http://www.nilim.go.jp/lab/bcg/siryou/tnn/tnn0485.htm⟩. 2013, (in Japanese).

Peregrine DH. Water –wave impact on walls. *Annual Review of Fluid Mechanics*, 2003, 35, 23-43.

PHB. Technical Standards and Commentaries for Port and Harbour Facilities in Japan. ⟨http://www.mlit.go.jp/kowan/kowan_tk5_000017.html⟩. 2014, (in Japanese).

Raby A. Macabuag J. Pomonis A. Wilkinson S. and Rossetto T. Implications of the 2011 Great East Japan Tsunami on Sea Defence Design. *International Journal of Disaster Risk Reduction*, 2015, 14, 332-346.

Roberston IN, Paczkowski K. Riggs HR. and Mohamed A. Experimental investigation of tsunami bore forces on vertical walls. *Journal of Offshore Mechanics and Arctic Engineering*, 2013, 135.

Rossetto T, Allsop W, Charvet I, and Robinson DI. Physical modelling of tsunami using a new pneumatic wave generator. *Coastal Engineering*, 2011, 58; 517-527.

Shibayama T, Esteban M, Nistor I, Takagi H, Danh Thao N, Matsumaru R, Mikami T, Aranguiz R, Jayaratne R, and Ohira K. Classification of tsunami and evacuation areas. *Natural Hazards*, 2013, 67; 365-386

Yeh H., Maximum fluid forces in the tsunami runup zone. *Journal of Waterway Port and Coastal Ocean Engineering*. 2006, 132 (6), 496–500.